Supporting Tables, Figures and Methods

Supplemental Table S1. Candidate genes selected.

Gene Name	Gene symbol	References
Genes that play, or are assumed to play, a role in lycopene and triglyceride metabolism in adipose tissue		
β-carotene 15,15'oxygenase-1	*BCO1*	[1]
β-carotene 9,10' oxygenase-2	*BCO2*	[2]
Cluster of Differentiation 36	*CD36*	[3]
ELOVL fatty acid elongase 5	*ELOVL5*	[4]
GRAM domain containing 1A	*GRAMD1A*	[5,6]
GRAM domain containing 1C	*GRAMD1C*	[5,6]
Low density lipoprotein receptor	*LDLR*	[7]
Lipase E	*LIPE*	[8]
Lipoprotein lipase	*LPL*	[9]
Monoglyceride lipase	*MGLL*	[10,11]
Polycystic kidney disease 1-like 2	*PKD1L2*	[1]
Patatin-like Phospholipase Domain-containing 2	*PNPLA2*	[8]
Peroxisome proliferator activated receptor gamma	*PPARG*	[12]
Scavenger receptor class B member 1	*SCARB1*	[13]
Genes whose SNPs have been associated with circulating lycopene concentration in GWAS		
ATP binding cassette subfamily B member 1	*ABCB1*	[14]

Retinol dehydrogenase 12	*RDH12*	[15]
SET domain containing 7	*SETD7*	[16]

Genes whose SNPs have been associated with the postprandial chylomicron lycopene or triacylglycerol response in the same group of participants

ATP binding cassette subfamily G member 2	*ABCG2*	[17,18]
ATP binding cassette subfamily A member 1	*ABCA1*	[17–20]
ATP binding cassette subfamily G member 5	*ABCG5*	[19]
Apolipoprotein A1	*APOA1*	[18]
Apolipoprotein A3	*APOA3*	[18]
Apolipoprotein A4	*APOA4*	[18]
Apolipoprotein A5	*APOA5*	[18,20]
Apolipoprotein B	*APOB*	[17–19]
COBL-like 1	*COBLL1*	[18]
Chemokine (C-X-C motif) ligand 8	*CXCL8*	[19]
ELOVL fatty acid elongase 2	*ELOVL2*	[17–19]
Fatty acid desaturase 1	*FADS1*	[21]
Fatty acid desaturase 2	*FADS2*	[21]
Fatty acid desaturase 3	*FADS3*	[21]
Insulin induced gene 2	*INSIG2*	[17,18]
Insulin receptor substrate 1	*IRS1*	[18]
Intestine specific homebox	*ISX*	[17–19,21]
Lipase, hepatic	*LIPC*	[17–19]

Melanocortin 4 receptor	*MC4R*	[18]
Microsomal triglyceride transfer protein	*MTTP*	[17,18]
Niemann-Pick disease, type C1, gene-like 1	*NPC1L1*	[17]
Pancreatic lipase	*PNLIP*	[17]
Retinal pigment epithelium-specific protein 65kDa	*RPE65*	[18,19]
Solute carrier family 27, member 6	*SLC27A6*	[17]
Superoxide dismutase 2, mitochondrial	*SOD2*	[17,19]
Transcription factor 7 like 2	*TCF7L2*	[19]

Supplemental Table S2A-B. Comparison between adipose tissue lycopene concentrations measured at fast and 8 h after consumption of the 3 test meals.

A. Linear mixed model

Parameters[a]	Numerator *df*	Denominator *df*	F	Sig.
Intercept	1	39.1	147.2	0.000
Sampling time (Fasting vs 8 h)	1	41.5	0.6	0.435
Type of Meal (Control vs Vitamin E vs Tomato Puree)	2	35.0	0.9	0.433
Time * Type of Meal	2	38.7	1.7	0.188

[a]Unstructured linear mixed model. Adipose tissue lycopene concentrations measured at fast and 8 h after consumption of the 3 test meals were analyzed with linear mixed models, using a full factorial design with meal (control, vitamin E and tomato puree) and time (fasting and 8 h post-meal) as fixed within-subject variables and participant as the random variable. Of the 5 linear mixed models tested, the unstructured model was selected based on Akaike's Information Criterion [22]

B. Paired *t*-test

Type of Meal	Paired Differences					*t*	df	Sig.
	Mean	SD	SEM	95% CI				
				Lower	Upper			
Control Meal	-23.7	286.5	49.1	-123.6	76.3	-0.5	33	0.6
Vitamin E Meal	20.3	290.5	51.3	-84.4	125.0	0.4	31	0.7
Tomato Puree Meal	78.2	319.3	53.2	-29.9	186.2	1.5	35	0.2

Abbr: df, degrees of freedom; sig, significance (*p*-value) for paired *t*-test.

Supplemental Table S3. Characteristics of the partial least squares regression models generated.

Number of predictors	R^2	**Adjusted** R^2	R^2 **after 100 permutations**[b]	R^2 **after cross-validation**[c]	**Cross-validation-ANOVA** *p*-**value**[c]
100[a]	0.85	1.11	0.53	0.79	4.18×10^{-14}
36	0.79	-0.51	0.31	0.73	4.76×10^{-12}
30	0.77	0.19	0.27	0.70	2.63×10^{-11}
23	0.75	0.45	0.27	0.69	5.75×10^{-11}
20	0.74	0.50	0.25	0.68	1.20×10^{-10}
19	0.73	0.51	0.26	0.67	2.02×10^{-10}
18	0.73	0.53	0.24	0.67	2.58×10^{-10}
17	**0.73**	**0.55**	**0.24**	**0.67**	$\mathbf{1.98 \times 10^{-10}}$
16	0.72	0.54	0.22	0.66	5.58×10^{-10}
14	0.69	0.54	0.19	0.62	3.28×10^{-9}
12	0.64	0.50	0.18	0.57	4.25×10^{-8}
10	0.60	0.48	0.16	0.53	2.79×10^{-7}
7	0.52	0.42	0.12	0.40	3.76×10^{-5}
5	0.49	0.42	0.08	0.34	2.47×10^{-4}
3	0.38	0.33	0.06	0.32	4.64×10^{-4}

The selected model is highlighted in bold font. All models had one component.

[a] Model 1 includes fasting concentrations for HDL-C, total cholesterol and lycopene.

[b]See **Supplemental Figure S3** for further explanation of the procedure.

[c]See [23].

Supplemental Figure S1. Candidate SNP selection flowchart.

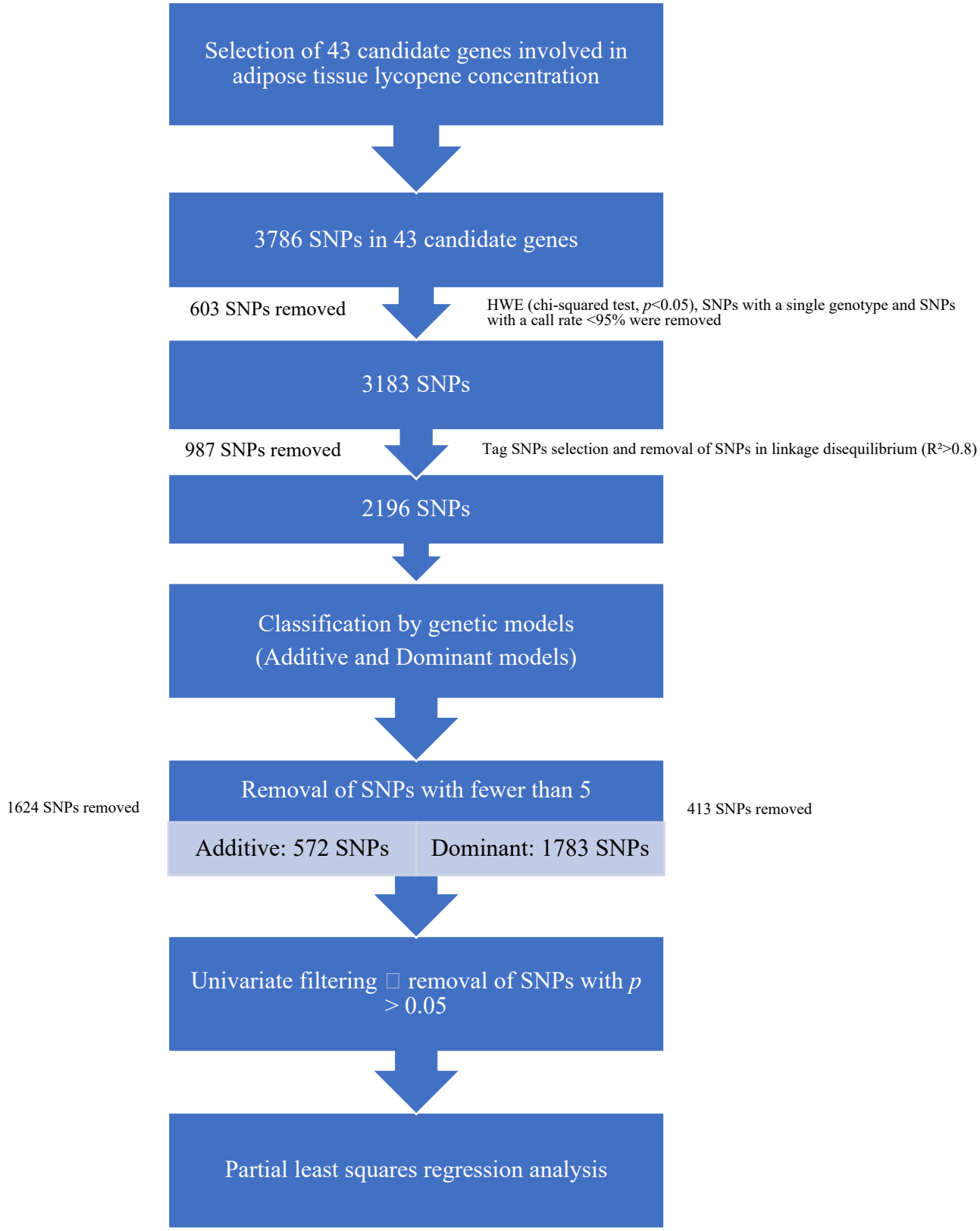

Supplemental Information: additional validations of the partial least squares (PLS) regression model.

1) Leave-k-*out* cross-validation

The leave *k*-out validation procedure was based on Steyerberg *et al.* [24]. We tested the robustness of our PLS regression model by randomly excluding k number of participants (k = 1, 2, 3, 4) from the original dataset, creating a training set. The excluded participants were then reintroduced to assess whether models trained without them could accurately predict their adipose tissue lycopene concentrations. This process was repeated for each participant, ensuring each was left out once (i.e., 43 times for k=1, 21 times for k=2, 14 times for k=3, and 10 times for k=4).

The average relative prediction errors for the leave-k-out procedure are presented in **Supplemental Table S4**. The error percentage remained relatively consistent, even when up to 4 participants were left out, indicating that the PLS regression model was fairly robust.

Supplemental Table S4. Average relative prediction error following the leave-*k*-out procedure.

	Number of participants left out				
	0	1	2	3	4
%error	32.7	37.0	32.8	36.6	37.7

*2) Regression coefficient stability testing following the leave-*k*-out procedure*

We checked that the regression coefficients of the 17 SNPs from the selected model (**Table 3**) remained unchanged ($p>0.05$; ANOVA) following the leave-*k*-out procedure described above. **Supplemental Figure S2** shows good stability of the regression coefficients with this validation.

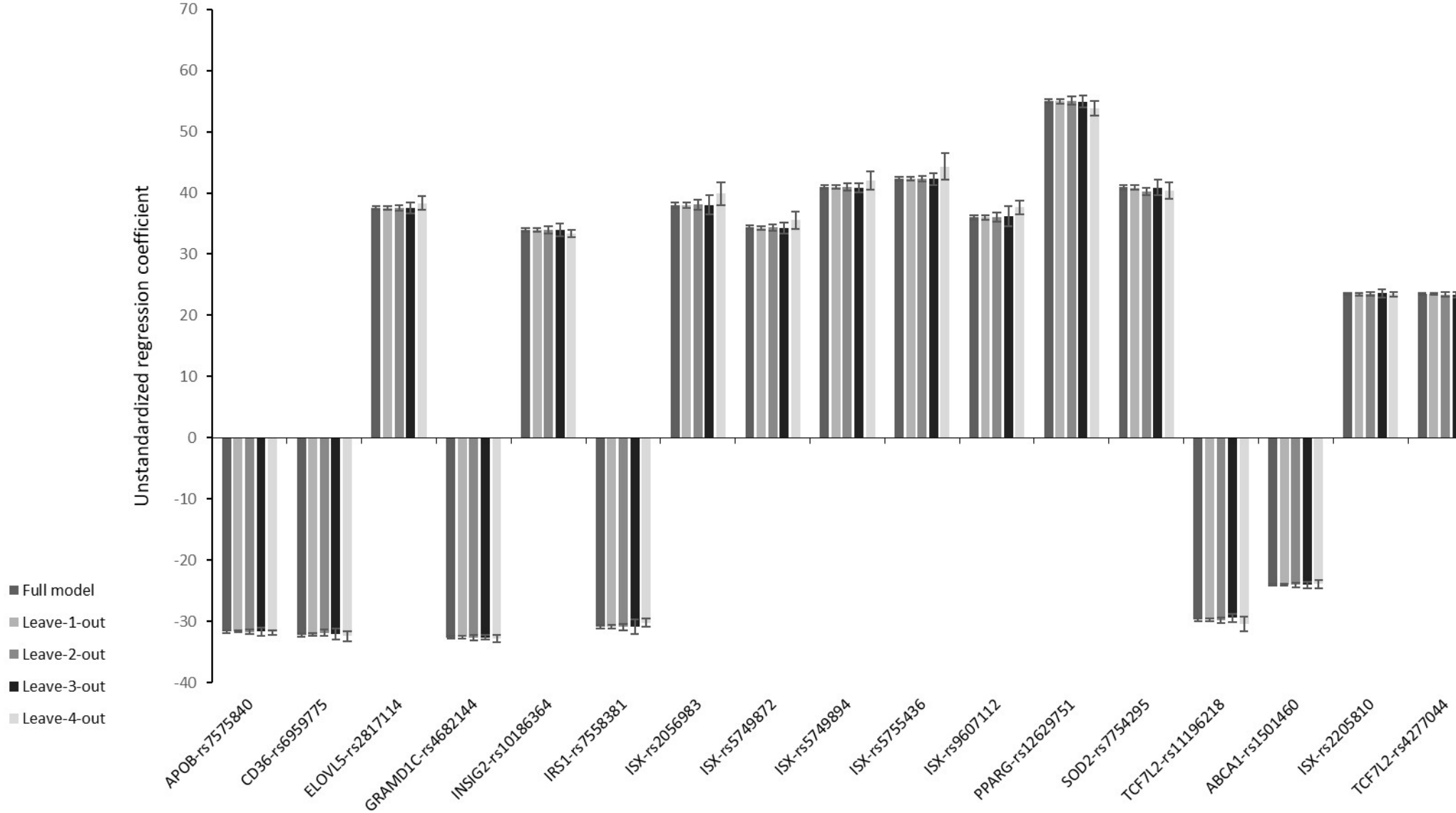
Unstandardized regression coefficient
70
60
50
40
30
20
10
0
-10
-20
-30
-40
Full model
Leave-1-out
Leave-2-out
Leave-3-out
Leave-4-out
APOB-rs7575840
CD36-rs6959775
ELOVL5-rs2817114
GRAMD1C-rs4682144
INSIG2-rs10186364
IRS1-rs7558381
ISX-rs2056983
ISX-rs5749872
ISX-rs5749894
ISX-rs5755436
ISX-rs9607112
PPARG-rs12629751
SOD2-rs7754295
TCF7L2-rs11196218
ABCA1-rs1501460
ISX-rs2205810
TCF7L2-rs4277044

Supplemental Figure S2: SNPs stability following the leave-*k*-out procedure. *k* participants (k = 1, 2, 3, 4) were randomly excluded from the original dataset, creating a training subset. These participants were then reintroduced into the training set to assess the regression coefficients of the 17 SNPs in the selected model. This process was repeated so that each participant was excluded once. One-way ANOVA performed on each gene showed no significant differences between the full model and the four training subsets generated. Gene names are provided in **Supplemental Table S1.**

3) R^2 *and adjusted* R^2 *of the selected model after 100 permutations.*

This procedure 1) evaluates the risk that the PLS regression model is spurious, meaning it fits the current dataset well but fails to predict Y accurately for new observations, and 2) checks for overfitting. To assess overfitting, the accuracy of the original model (measured by R^2 and R^2 after cross-validation) was compared with the accuracy of 100 models generated by randomly permuting the order of the Y matrix (adipose tissue lycopene concentration) for the participants, while keeping the X matrix (genotypes at the selected SNPs) unchanged. A robust model should never predict the permuted Y variables using the intact X variables. The results of these permutations for the selected PLS regression model are shown in **Supplemental Figure S3.**

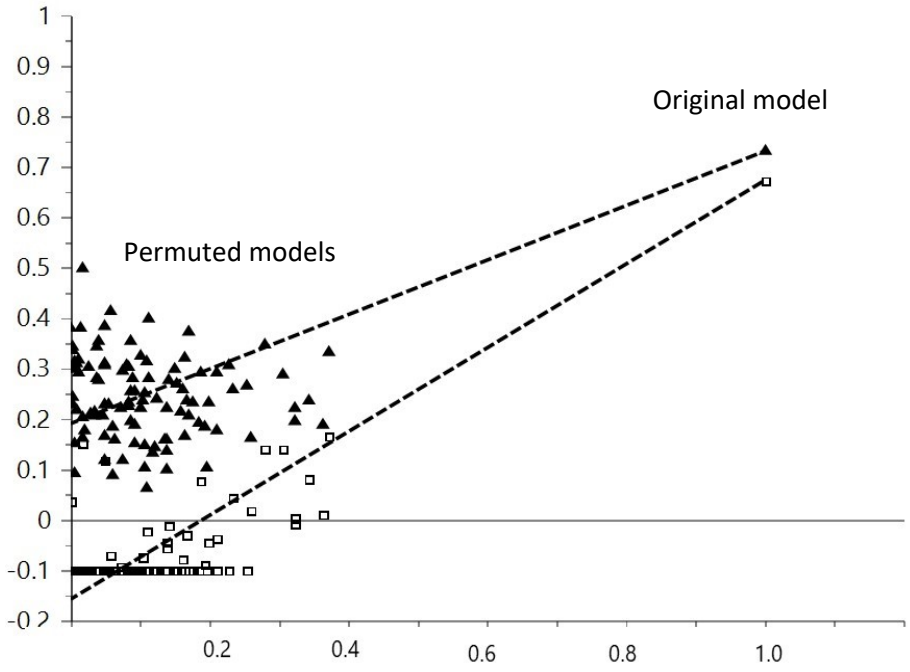

Supplemental Figure S3. The horizontal axis represents the correlation between the permuted *Y*'s and the original *Y*'s. The vertical axis represents the R^2 (dashed line and black triangles) and R^2 after cross-validation (dashed line and squares) values obtained in the permuted models.

Values of the original model are on the far right (at correlation = 1), values of the 100 *Y*-permuted models are further to the left. The average R^2 after 100 permutations was 0.24. This strongly supports the conclusion that the ability of the original, non-permuted model, to predict the adipose tissue lycopene concentration is not due to chance.

References:

[1] M.L. Bonet, J. Ribot, S. Galmés, F. Serra, A. Palou, Carotenoids and carotenoid conversion products in adipose tissue biology and obesity: Pre-clinical and human studies, Biochim Biophys Acta Mol Cell Biol Lipids 1865 (2020) 158676. https://doi.org/10.1016/j.bbalip.2020.158676.

[2] J. Amengual, G.P. Lobo, M. Golczak, H.N.M. Li, T. Klimova, C.L. Hoppel, A. Wyss, K. Palczewski, J. von Lintig, A mitochondrial enzyme degrades carotenoids and protects against oxidative stress, FASEB J 25 (2011) 948–959. https://doi.org/10.1096/fj.10-173906.

[3] C.C. Allred, T. Krennmayr, C. Koutsari, L. Zhou, A.H. Ali, M.D. Jensen, A novel ELISA for measuring CD36 protein in human adipose tissue, J Lipid Res 52 (2011) 408–415. https://doi.org/10.1194/jlr.M008995.

[4] H. Guillou, D. Zadravec, P.G.P. Martin, A. Jacobsson, The key roles of elongases and desaturases in mammalian fatty acid metabolism: Insights from transgenic mice, Prog Lipid Res 49 (2010) 186–199. https://doi.org/10.1016/j.plipres.2009.12.002.

[5] S. Bandara, J. Moon, S. Ramkumar, J. von Lintig, ASTER-B regulates mitochondrial carotenoid transport and homeostasis, J Lipid Res 64 (2023) 100369. https://doi.org/10.1016/j.jlr.2023.100369.

[6] S. Bandara, S. Ramkumar, S. Imanishi, L.D. Thomas, O.B. Sawant, Y. Imanishi, J. von Lintig, Aster proteins mediate carotenoid transport in mammalian cells, Proc Natl Acad Sci U S A 119 (2022) e2200068119. https://doi.org/10.1073/pnas.2200068119.

[7] M.S.F. Lavrador, M.S. Afonso, D.E. Cintra, M. Koike, V.S. Nunes, M. Demasi, C.J. Lin, L.M.M. Beda, L.A. Gioielli, R. de P.A. Bombo, R.M. Machado, S. Catanozi, E.R. Nakandakare, A.M. Lottenberg, Interesterified Fats Induce Deleterious Effects on Adipose Tissue and Liver in LDLr-KO Mice, Nutrients 11 (2019) 466. https://doi.org/10.3390/nu11020466.

[8] X. Zhang, C.C. Zhang, H. Yang, K.G. Soni, S.P. Wang, G.A. Mitchell, J.W. Wu, An Epistatic Interaction between Pnpla2 and Lipe Reveals New Pathways of Adipose Tissue Lipolysis, Cells 8 (2019) 395. https://doi.org/10.3390/cells8050395.

[9] R. Zechner, J. Strauss, S. Frank, E. Wagner, W. Hofmann, D. Kratky, M. Hiden, S. Levak-Frank, The role of lipoprotein lipase in adipose tissue development and metabolism, Int J Obes Relat Metab Disord 24 Suppl 4 (2000) S53-56. https://doi.org/10.1038/sj.ijo.0801506.

[10] J.Z. Long, B.F. Cravatt, The metabolic serine hydrolases and their functions in mammalian physiology and disease, Chem Rev 111 (2011) 6022–6063. https://doi.org/10.1021/cr200075y.

[11] R. Zechner, P.C. Kienesberger, G. Haemmerle, R. Zimmermann, A. Lass, Adipose triglyceride lipase and the lipolytic catabolism of cellular fat stores, J Lipid Res 50 (2009) 3–21. https://doi.org/10.1194/jlr.R800031-JLR200.

[12] A. Koppen, E. Kalkhoven, Brown vs white adipocytes: the PPARgamma coregulator story, FEBS Lett 584 (2010) 3250–3259. https://doi.org/10.1016/j.febslet.2010.06.035.

[13] L. Yvan-Charvet, A. Bobard, P. Bossard, F. Massiéra, X. Rousset, G. Ailhaud, M. Teboul, P. Ferré, G. Dagher, A. Quignard-Boulangé, In vivo evidence for a role of adipose tissue SR-BI in the nutritional and hormonal regulation of adiposity and cholesterol homeostasis, Arterioscler Thromb Vasc Biol 27 (2007) 1340–1345. https://doi.org/10.1161/ATVBAHA.106.136382.

[14] N.E. Moran, J.M. Thomas-Ahner, J.L. Fleming, J.P. McElroy, R. Mehl, E.M. Grainger, K.M. Riedl, A.E. Toland, S.J. Schwartz, S.K. Clinton, Single nucleotide polymorphisms in β-carotene oxygenase 1 are associated with plasma lycopene responses to a tomato-

soy juice intervention in men with prostate cancer, The Journal of Nutrition 149 (2019) 381–397.
[15] I. Domarkienė, A. Mažeikienė, G. Petrauskaitė, Z.A. Kučinskienė, V. Kučinskas, New associations of serum β-carotene, lycopene, and zeaxanthin concentrations with NR1H3, APOB, RDH12, AND CYP genes, Food Sci Nutr 10 (2022) 763–771. https://doi.org/10.1002/fsn3.2705.
[16] C.R. D'Adamo, A. D'Urso, K.A. Ryan, L.M. Yerges-Armstrong, R.D. Semba, N.I. Steinle, B.D. Mitchell, A.R. Shuldiner, P.F. McArdle, A common variant in the SETD7 gene predicts serum lycopene concentrations, Nutrients 8 (2016) 82–82.
[17] P. Borel, C. Desmarchelier, M. Nowicki, R. Bott, Lycopene bioavailability is associated with a combination of genetic variants, Free Radical Biology and Medicine 83 (2015) 238–244. https://doi.org/10.1016/j.freeradbiomed.2015.02.033.
[18] P. Borel, C. Desmarchelier, M. Nowicki, R. Bott, S. Morange, N. Lesavre, Interindividual variability of lutein bioavailability in healthy men: characterization, genetic variants involved, and relation with fasting plasma lutein concentration, The American Journal of Clinical Nutrition 100 (2014) 168–175. https://doi.org/10.3945/ajcn.114.085720.
[19] P. Borel, C. Desmarchelier, M. Nowicki, R. Bott, A Combination of Single-Nucleotide Polymorphisms Is Associated with Interindividual Variability in Dietary β-Carotene Bioavailability in Healthy Men, The Journal of Nutrition 145 (2015) 1740–1747. https://doi.org/10.3945/jn.115.212837.
[20] C. Desmarchelier, J.-C. Martin, R. Planells, M. Gastaldi, M. Nowicki, A. Goncalves, R. Valéro, D. Lairon, P. Borel, The postprandial chylomicron triacylglycerol response to dietary fat in healthy male adults is significantly explained by a combination of single nucleotide polymorphisms in genes involved in triacylglycerol metabolism, The Journal of Clinical Endocrinology & Metabolism 99 (2014) E484–E488.
[21] M.P. Zumaraga, P. Borel, R. Bott, M. Nowicki, D. Lairon, C. Desmarchelier, The Interindividual Variability of Phytofluene Bioavailability is Associated with a Combination of Single Nucleotide Polymorphisms, Mol Nutr Food Res (2022) 2200580. https://doi.org/10.1002/mnfr.202200580.
[22] H. Bozdogan, Model selection and Akaike's Information Criterion (AIC): The general theory and its analytical extensions, Psychometrika 52 (1987) 345–370. https://doi.org/10.1007/BF02294361.
[23] L. Eriksson, J. Trygg, S. Wold, CV-ANOVA for significance testing of PLS and OPLS® models, Journal of Chemometrics: A Journal of the Chemometrics Society 22 (2008) 594–600.
[24] E.W. Steyerberg, F.E. Harrell Jr, G.J.J.M. Borsboom, M.J.C. Eijkemans, Y. Vergouwe, J.D.F. Habbema, Internal validation of predictive models: efficiency of some procedures for logistic regression analysis, J Clin Epidemiol 54 (2001) 774–781.